

Evidence for significant backscattering in near-threshold electron-impact excitation of $\text{Ar}^{7+}(3s \rightarrow 3p)$

X. Q. Guo, E. W. Bell, J. S. Thompson,* and G. H. Dunn[†]
*Joint Institute for Laboratory Astrophysics of the University of Colorado
 and the National Institute of Standards and Technology, Boulder, Colorado 80309*

M. E. Bannister and R. A. Phaneuf*
Oak Ridge National Laboratory, Oak Ridge, Tennessee 37831-6372

A. C. H. Smith
University College London, London WC1E 6BT, United Kingdom

(Received 29 July 1992)

Measurements of absolute total cross sections for electron-impact excitation of $\text{Ar}^{7+}(3s \rightarrow 3p)$ using a merged-beams electron-energy-loss technique show that near threshold the inelastically scattered electrons are ejected primarily in the backward direction. This unusual angular scattering has not been previously observed for atoms or ions, but may be typical for multiply charged ions. The total cross sections, measured over an energy range to 2.2 eV above threshold, agree with seven-state *R*-matrix close-coupling calculations. Both close-coupling and distorted-wave calculations also confirm the backscattering observed in these measurements.

PACS number(s): 34.80.Kw

In this Rapid Communication we report experimental observations of significant (over 90%) backward inelastic electron scattering during electron-impact excitation of the sodiumlike ion, $\text{Ar}^{7+}(3s \rightarrow 3p)$, near the excitation threshold. We believe that such backscattering has not been previously observed. A special merged-beams configuration [1,2] makes it possible to separate inelastically scattered electrons traveling forward and backward in the laboratory frame, and hence to infer gross features of the differential scattering in the center of mass (c.m.) frame.

Excitation of multiply charged ions by electron impact enters intimately into the modeling and diagnostics of high-temperature plasmas such as those encountered in astrophysics and controlled fusion. It is unimaginable that the millions of cross sections needed for such modeling could be measured, but accurate experiments on excitation cross sections of relevant ions are needed as benchmarks for testing the theoretical methods used to compute such cross sections. However, a conspicuous paucity of experimental data exists [3].

For multiply charged ions, excitation cross sections for resonance transitions in C^{3+} , N^{4+} , Al^{2+} , and Ba^{46+} have been measured by detecting the emitted photons [4]. Absolute total excitation cross sections for $\text{Si}^{3+}(3s \rightarrow 3p)$ have been measured [1] recently by Wählin *et al.* using the merged-beams energy-loss technique used here. A similar technique has been used [5] for cross-section measurements on the singly charged ion, Mg^+ . Measurements of inelastic differential cross sections (DCS's) are even more limited. The only measurements on multiply charged ions to date have been made by Huber *et al.* [6] for $\text{Ar}^{7+}(3s \rightarrow 3p)$ for electron scattering angles from 13° to 29° at an energy of 100 eV. The DCS peaks at about

20° . Results for three singly charged ions, Zn^+ , Mg^+ , and Cd^+ , have been reported [7] for $4^\circ < \theta < 17^\circ$ for energies well above the excitation threshold. The measured DCS's were also peaked in the forward direction for the energies investigated. No DCS measurements have been reported on any ions near the excitation threshold [3].

Using the merged-beams apparatus, at energies close to the excitation threshold, the angular distribution of the inelastically scattered electrons in the laboratory frame is very sensitive to the ion velocity because of the transformation of scattering angle between the c.m. and laboratory frames. When the scattering is in the backward direction ($\theta' > 90^\circ$) in the c.m. frame, the ion beam velocity can be adjusted to make these scattered electrons travel either forward or backward in the laboratory frame. That portion of the electrons scattered backward (or with very small forward velocities) in the laboratory frame will not reach the detector, resulting in a reduction of the observed total cross section. By measuring the dependence of the apparent cross section σ_{app} on ion velocity, we are able to infer significant (over 90%) backscattering for excitation of Ar^{7+} near the excitation threshold. Our experimental evidence for backscattering has recently been confirmed independently by both close-coupling [8] (CC) and distorted-wave [9] (DW) calculations. We also present measurements here of the absolute total excitation cross sections for $\text{Ar}^{7+}(3s \rightarrow 2p)$ in an energy range extending to 2.2 eV above the mean excitation threshold of 17.59 eV and we compare our data with recent calculations [10].

Descriptions of the merged-beams electron-energy-loss apparatus have been reported previously [1,2], and only a brief overview can be presented here. The apparatus is immersed in a uniform solenoidal magnetic field (≈ 3.3

mT) parallel to the incident ion beam. Electrons from an electron gun are focused into the space between a pair of parallel plates (the merger) producing a transverse electric field of about 10 V/mm. In the crossed E and B fields of the merger, the electrons execute trochoidal motion, which can be viewed as cyclotron motion about the B field and drift perpendicular to the two fields with velocity $\mathbf{v}_d = \mathbf{E} \times \mathbf{B} / B^2$. Thus, after an integral number n of cyclotron periods T , the initial velocity of the electrons is reproduced at the exit of the merger, but the particles are displaced perpendicular to the two field directions by an amount $(E/B)nT$ (for our case, $n=2$). Multiply charged ions from the Oak Ridge National Laboratory ECR ion source are merged with the electrons at the merger exit. Ions and electrons then travel together in an electric-field-free region (about 63 mm long) where the collisions take place. At the end of this collision region, the primary electrons and inelastically scattered electrons are separated by the action of a second pair of parallel plates (the demerger) with an electric field of about 2.5 V/mm. The demerger acts as an energy dispersion device [1,2,5]. Unscattered electrons, deflected by the demerger through a relatively small angle, are collected by a Faraday cup, while inelastically scattered electrons, deflected through much larger angles, strike a position-sensitive detector (PSD) oriented with its plane normal to the $\mathbf{E} \times \mathbf{B}$ direction. The operating pressure is about 1.5×10^{-8} Pa.

The measurement of the extent of electron- and ion-beam overlap (form factor) along the merge path is accomplished using a movable beam probe [11] employing fluorescent screen and digitized video techniques. This device permits direct viewing of the overlaps of the electron and ion beams. The overlap was optimized in the “upstream” portion of the merge path and “spoiled” near the entrance to the demerger. This minimizes elastic scattering of electrons by ions where they could be detected [1] with the same temporal and spatial signatures of inelastically scattered electrons. The signal-to-background ratio was always less than 10^{-2} , necessitating chopping both beams at 2000 Hz in a phased four-way chopping sequence [1,2] to extract the signal. The signal rate at each pixel of the PSD (256×64 pixels) was recorded and the spatial distribution of the inelastically scattered electrons at the plane of the PSD was displayed.

The excitation cross section was determined from the expression

$$\sigma(E_{\text{c.m.}}) = \frac{R}{\epsilon} \left| \frac{v_e v_i}{v_e - v_i} \right| \frac{q e^2}{I_e I_i} F, \quad (1)$$

where R is the count rate from detection of inelastically scattered electrons by the PSD, ϵ the measured PSD detection efficiency, F the form factor, and v_e, v_i, I_e, I_i are the velocities and currents of the electrons and ions of charge qe , respectively. Typically, the signal rate was between 10 and 80 Hz, and the electron and ion background rates were 40 and 130 Hz/nA, respectively. At typical electron and ion currents of 200 and 50 nA, the dead-time correction for the PSD counts was $(8 \pm 0.16)\%$. The typical ion-beam diameter was 1.5 mm after collima-

tion; the electron beam was confined within a diameter of 2.5 mm. The form factor F was typically around 0.025 mm. In taking data at a desired energy in the center of mass, $E_{\text{c.m.}}$, a convenient electron energy was chosen and the beam was optimized for background, shape, and trajectory. The simple relationship between the c.m. and laboratory systems was used to obtain the necessary laboratory energy for the ions. The relevant variables in Eq. (1) were, of course, independently measured for each point.

The measured absolute total excitation cross sections for the $\text{Ar}^{7+}(3s \rightarrow 3p)$ resonance transition are plotted in Fig. 1. The error bars represent the total relative uncertainty at a 90% confidence level (CL), a quadrature sum with contributions of 12% from statistical counting uncertainty, 6% from form factors, and 7% from spatially delimiting the signal on the PSD pictures. The absolute uncertainty at similar CL's (we call this combination of statistical and systematic uncertainties at a high confidence level, HCL), in addition, includes systematic uncertainties of 12% from the form factor, 3% from the PSD dead-time correction, 3% from the PSD efficiency and 1% each from the electron and ion currents. The typical HCL total absolute uncertainty is about 20%, indicated in Fig. 1 by double error bars on the single data point at 18.62 eV.

The solid line in Fig. 1 represents results of the R -matrix seven-state close-coupling calculations of Badnell, Pindzola, and Griffin [10]. The agreement between theory and experiment is good over the entire energy range investigated. The data points between 17.4 to 17.9 eV are least-squares fitted to the convolution of two suc-

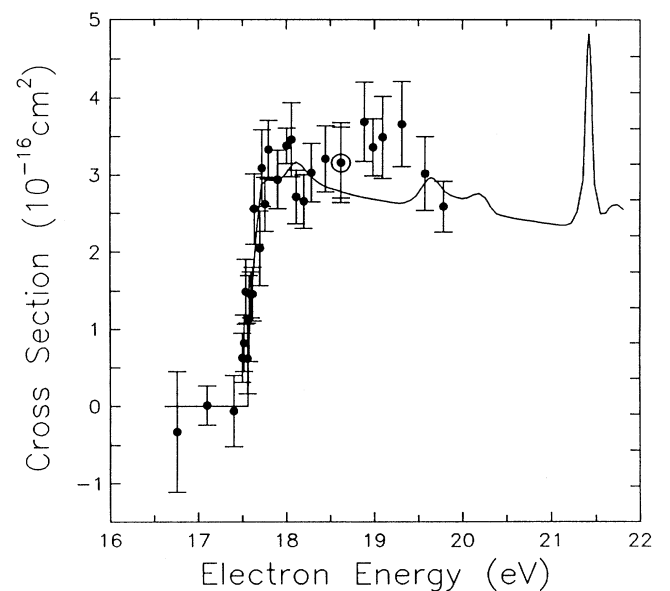


FIG. 1. The measured total absolute cross sections for electron-impact excitation of $\text{Ar}^{7+}(3s \rightarrow 3p)$. The solid curve represents a seven-state close-coupling R -matrix calculation (Ref. [10]) after convolution with an electron-energy distribution of 0.2 eV in FWHM. The error bars denote relative uncertainties at a 90% CL. The outer error bar on the 18.62-eV point represents the HCL total absolute uncertainty.

cessive step functions representing excitation to the $P_{1/2}$ and $P_{3/2}$ states (thresholds at 17.36 and 17.70 eV, respectively) with a Gaussian electron-energy distribution. The fitting yields an electron-energy spread of 0.2 eV full width at half maximum (FWHM) and a threshold excitation cross section of $3.0 \times 10^{-16} \text{ cm}^2$. The FWHM energy spread value is consistent with that obtained from the Si^{3+} experiment [1].

As already mentioned, the measured *apparent* cross sections σ_{app} depend on the ion velocity and the DCS. To observe the dependence, σ_{app} was measured at a fixed electron energy (27.15 eV) as a function of the ion energy ranging from 58 to 72 keV, with a corresponding range of $E_{\text{c.m.}}$ from 1.06 to 0.2 eV above the excitation threshold. Clearly, if one collects all of the scattered electrons, one expects to reproduce the cross section shown in Fig. 1 over the relevant energy range. The velocity of the center of mass, $V_{\text{c.m.}}$ (to a very good approximation, the velocity of the ions) ranges from $(5.29\text{--}5.90) \times 10^5 \text{ ms}^{-1}$ over this ion energy range. At the threshold for excitation, the scattered electrons have zero velocity in the c.m. frame and $V_{\text{c.m.}}$ in the laboratory frame. At greater energies, the electron velocity in the laboratory frame is the vector sum of the electron velocity v'_e of the scattered electrons in the c.m. frame and $V_{\text{c.m.}}$. Clearly, when $V_{\text{c.m.}} + v'_e \cos \theta' < 0$, where θ' is the scattering angle in the c.m. frame, the resultant electron velocity in the laboratory frame will be in the backward direction, and the electron will not reach the detector. The range of v'_e for this study was $(2.65\text{--}6.1) \times 10^5 \text{ ms}^{-1}$; so there was ample opportunity to observe backward scattering for the given $V_{\text{c.m.}}$. Figure 2 shows σ_{app} plotted versus E_{ion} , and the falling off of σ_{app} with decreasing E_{ion} is clear evidence for backscattering. At each $E_{\text{c.m.}}$ where signal was lost, it could be retrieved by increasing E_{ion} enough and adjusting E_{el} to obtain the same $E_{\text{c.m.}}$, so that the accurate data of Fig. 1 could be obtained. Signal loss similar to that in Fig. 2 for electron energies other than 27.15 eV was also observed.

The backscattering evidenced in the present investigation has been confirmed by theory. The inset of Fig. 2 illustrates the theoretical differential cross sections $d\sigma/d\theta'$ calculated in both the close-coupling [8] (solid curve) and distorted-wave [9] (dashed curve) approximations. The CC curve is for $E_{\text{c.m.}}$ 1.27 eV above threshold, while the DW curve is for $E_{\text{c.m.}}$ 1.41 eV above threshold. The CC differential cross sections at 0.27 and 2.27 eV above threshold are essentially the same as that shown, and the backscattering does not seem to be associated with resonance effects.

The solid curves in Fig. 2 represent the expected σ_{app} versus E_{ion} for three different angular distributions: Curve *a* is for the backscattered electrons illustrated by the solid curve in the inset and as calculated in the CC approximation [8], curve *b* is for an isotropic distribution of scattered electrons, and curve *c* is for a forward-peaked distribution [12]. The curves were obtained using a charged-particle trajectory program, approximating the geometry of our electrode configuration, and incorporating the three angular distributions described. In each

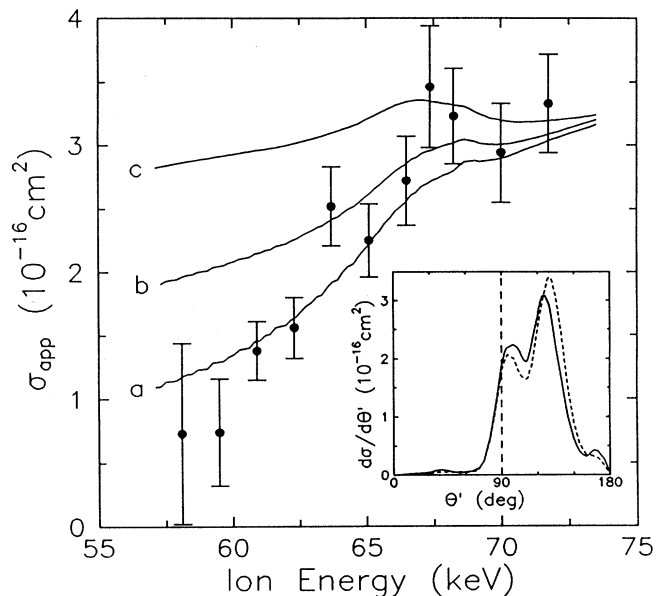


FIG. 2. Measured apparent cross sections as a function of laboratory ion energy and for fixed laboratory electron energy of 27.15 eV. Error bars are 90% CL. Solid curves from modeling (see text) using relative differential scattering cross sections from (a) close-coupling calculations [solid curve, inset (Ref. [8])], (b) isotropic, (c) partial-wave calculations (Ref. [12]) with forward-peaked DCS. The total cross section for all three cases is as shown by the solid curve in Fig. 1. Inset, DCS from close-coupling (full curve, Ref. [8]) and distorted-wave (dashed curve, Ref. [9]) calculations.

case a single angular distribution was used (e.g., that at 1.27 eV above threshold for the CC curve), and the total cross section was taken as that represented by the solid curve in Fig. 1. The “hump” seen in each curve of Fig. 2, results from the small resonance seen in Fig. 1.

It is quite clear that only curve *a* agrees well with the measurements. Since neither an isotropic distribution nor anything more forward peaked than that comes close to describing the data, one must conclude that the scattering is dominantly in the backward direction. One could even speculate that the DCS may be even more strongly backward peaked than the theory predicts. Thus, we have observed strongly dominant backscattering of electrons inelastically scattered near threshold for excitation of $\text{Ar}^{7+}(3s \rightarrow 3p)$, and believe that these are the first observations of this phenomenon for excitation of any ion.

A physical feeling for the backscattering observed here can be obtained from a consideration of classical Coulomb trajectories. Consider electrons incident on Ar^{7+} with just enough energy (at infinity) to excite the ion (17.6 eV), and assume that the electrons excite the ion at the distance of closest approach r_c after gaining additional kinetic energy $7e^2/r_c$ in the field. The computed scattering angles under this assumption are *all* in the backward quadrant for $0.5a_0 \leq r_c \leq 25a_0$ (a_0 is the Bohr radius). If one imposes, as suggested by Huber *et al.* [6] in discussing their results at 100 eV, the further condition

that a unit of angular momentum is transferred at r_c , then r_c can be determined to be $3.4a_0$ and the scattering angle is 126.5° (compare inset of Fig. 2). The apparent validity of semiclassical theory at threshold may be rationalized by the fact that 12 or more partial waves contribute weakly to the CC and DW results at threshold [8,9].

We are grateful for the earlier collaboration of D.S. Belić, B.D. DePaola, J.L. Forand, D.C. Gregory, A. Müller, K. Rinn, D. Swenson, C.A. Timmer, and E.K. Wählin in the development of the merged-beams apparatus. We are also grateful to D.C. Griffin, N. Badnell, and M.S. Pindzola for providing the CC differential cross sections; to R.E.H. Clark for his DW calculations; and to

C. Bottcher for the partial-wave construction. This work was supported in part by the Office of Fusion Energy of the U.S. Department of Energy, under Contract No. DE-A105-86ER53237 with the National Institute of Standards and Technology and Contract No. DE-AC05-84OR21400 with Martin Marietta Energy Systems, Inc. M.E. Bannister acknowledges the support of the DOE Laboratory Cooperative Postgraduate Research Training Program administered by Oak Ridge Associated Universities. The authors would like to thank Professor Peng H-W for stimulating discussions. They are indebted to Professor Zheng W-M and Liu J-X for spotting out a numerical mistake in the early version of our paper. This work is partially supported by the Grant LWTZ-1298 of Chinese Academy of Science and The National Science Foundation of China.

*Present address: Department of Physics, University of Nevada, Reno, NV 89557.

†Quantum Physics Division, National Institute of Standards and Technology.

- [1] E. K. Wählin, J. S. Thompson, G. H. Dunn, R. A. Phaneuf, D. C. Gregory, and A. C. H. Smith, *Phys. Rev. Lett.* **66**, 157 (1991).
- [2] C. A. Timmer, Ph.D. thesis, University of Colorado, 1988 (unpublished); E. K. Wählin, Ph.D. thesis, University of Colorado, 1990 (unpublished).
- [3] G. H. Dunn, *Nucl. Fusion Suppl.: Atomic and Plasma-Material Interaction Data for Fusion* **2**, 25 (1992).
- [4] P. O. Taylor, D. C. Gregory, G. H. Dunn, R. A. Phaneuf, and D. H. Crandall, *Phys. Rev. Lett.* **39**, 1256 (1977); D. C. Gregory, G. H. Dunn, R. A. Phaneuf, and D. H. Crandall, *Phys. Rev. A* **20**, 410 (1979); D. S. Belić, R. A. Falk, G. H. Dunn, D. C. Gregory, and C. Cisneros, *Bull. Am. Phys. Soc.* **26**, 1315 (1981); R. E. Marrs, M. A. Levine, D. A. Knapp, and J. R. Henderson, *Phys. Rev. Lett.* **66**, 257 (1991).
- [5] S. J. Smith, K.-F. Man, R. J. Mawhorter, I. D. Williams, and A. Chutjian, *Phys. Rev. Lett.* **67**, 30 (1991).
- [6] B. A. Huber, C. Ristori, R. A. Hervieux, M. Maurel, and H. J. Andrä, *Phys. Rev. Lett.* **67**, 1407 (1991); C. Ristori, R. A. Hervieux, M. Maurel, H. J. Andrä, A. Brenac, J. Crançon, G. Lambole, Th. Lamy, P. Perrin, J. C. Rocco, F. Zadworny, and B. A. Huber, *Z. Phys. D* **22**, 425 (1991).
- [7] A. Chutjian, A. Z. Msezane, and R. J. W. Henry, *Phys. Rev. Lett.* **50**, 1357 (1983); A. Chutjian, *Phys. Rev. A* **29**, 64 (1984); I. D. Williams, A. Chutjian, and R. J. Mawhorter, *J. Phys. B* **19**, 2189 (1986).
- [8] D. C. Griffin, N. R. Badnell, and M. S. Pindzola (private communication).
- [9] R. E. H. Clark (private communication).
- [10] N. R. Badnell, M. S. Pindzola, and D. C. Griffin, *Phys. Rev. A* **43**, 2250 (1991).
- [11] J. L. Forand, C. A. Timmer, E. K. Wählin, B. D. DePaola, G. H. Dunn, D. Swenson, and K. Rinn, *Rev. Sci. Instrum.* **61**, 3372 (1990).
- [12] Peaked at $\theta=0^\circ$, half height at $\theta=34^\circ$ resulting from a partial-wave construction including partial waves only up to $l=2$. C. Bottcher (private communication).